coatings

MDPI

*Supplementary Materials*

# Fabrication of Nanostructures Consisting of Composite Nanoparticles by open-air PLD

**Anna Dikovska [1]*, Daniela Karashanova [2], Genoveva Atanasova [3], Georgi Avdeev [4], Petar Atanasov [1] and Nikolay Nedyalkov [1]**

[1] Institute of Electronics, Bulgarian Academy of Sciences, 72 Tsarigradsko Chaussee, 1784 Sofia, Bulgaria; dikovska@ie.bas.bg (A.D.); paatanas@ie.bas.bg (P.A.); nned@ie.bas.bg (N.N.)
[2] Institute of Optical Materials and Technologies "Acad. J. Malinowski", Bulgarian Academy of Sciences, Acad. G. Bonchev str., bl. 109, 1113 Sofia, Bulgaria; dkarashanova@yahoo.com (D.K)
[3] Institute of General and Inorganic Chemistry, Bulgarian Academy of Sciences, Acad. G. Bonchev str., bl. 11, 1113 Sofia, Bulgaria.; genoveva@svr.igic.bas.bg (Genoveva Atanasova)
[4] Rostislaw Kaischew Institute of Physical Chemistry, Bulgarian Academy of Sciences, Acad. G. Bonchev str., Bl.11, 1113 Sofia, Bulgaria; g_avdeev@ipc.bas.bg (Georgi Avdeev)
* Correspondence: dikovska@ie.bas.bg (A.D.)

## Results

*1. PLD of thin film*

1.1. PLD of pure Fe film

An XRD pattern of the thin film deposited from a pure Fe target is shown in Figure S1. The XRD analysis of the film revealed that its structure was crystalline and represented a combination of pure Fe and Fe-oxide phases (see Figure S1). The phase composition was identified as a cubic structure of bulk iron (Fe, ICSD 98-018-0971) and wüstite ($Fe_{1-x}O$, ICSD 98-002-7853). The estimated crystallite size of the iron and wüstite phases was about 31 and 15 nm, respectively. A precise study of the Fe film's structure allowed us to assume that the wüstite phase was probably formed on the glass substrate during the initial stage of deposition. The XRD analysis of the Fe-film performed at a grazing incidence configuration did not show any peaks associated with the wüstite phase of iron oxide. This result means that initially, the iron component ablated from the Fe target in vacuum formed an oxide phase reaching the glass substrate, on which, thereafter, the iron film started growing.

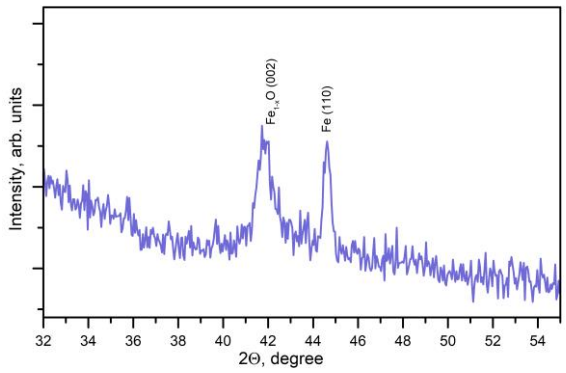


**Figure S1.** XRD pattern of the iron film.

The XPS analysis of the film surface was used to identify the surface chemical composition (see Figure S2). A high-resolution XPS spectrum of the Fe2p core level was deconvoluted into three doublet peaks. The film's binding energies for $Fe2p_{3/2}$ and $Fe2p_{1/2}$

were found to be 710.6 eV and 724.2 eV, respectively, with spin-orbit splitting of 13.6 eV. A satellite peak at about 719 eV was also detected, which is a specific peak associated with the $Fe^{3+}$ oxidation state [34]. The binding energy for Fe3p was estimated at ~ 55.6 eV, a peak value typical for the $Fe^{3+}$ oxidation state [34]. Bearing in mind all of the above, we concluded that the Fe atoms at the Fe film surface were in the $Fe^{3+}$ oxidation state (Figure S2).

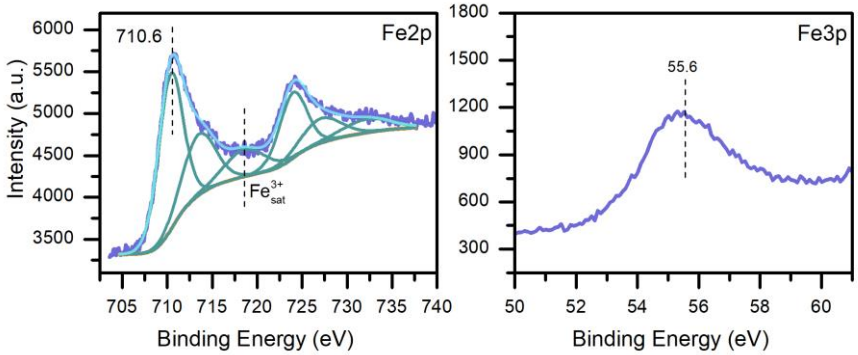


**Figure S2.** XPS spectra of the iron film.

*1.2. PLD of alloyed FeAu film*

An XRD pattern of the thin film deposited from a mosaic Fe–Au target is presented in Figure S3. The deposited film had a crystalline structure consisting of a pure Au phase (Au, ICSD 98-004-4362) and $Fe_{0.5}Au_{0.5}$ ($Fe_{0.5}Au_{0.5}$, ICSD 98-010-7985) alloy phase. Since the peak position of the alloy phase was shifted toward the Au peak, we used Vegard's law to estimate the precise FeAu alloy composition as being $Fe_{0.06}Au_{0.94}$. It could thus be concluded that the alloyed film phase composition was a combination of pure Au and Au-enriched FeAu alloy. The average crystallite size for the Au and Au-enriched FeAu alloy was determined as 45 nm and 5 nm, respectively. It should be noted that the position of the FeAu peak shifted with the change in the Fe: Au ratio of the mosaic target.

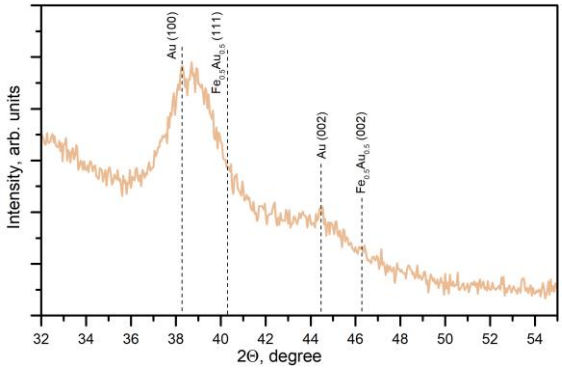


**Figure S3.** XRD pattern of the alloyed FeAu film.

Figure S4 shows the EDX spectrum of the FeAu film. The presence of Au and Fe elements are clearly observed. The estimated ratio of Fe: Au is approximately 1:2, as shown in Table 1.

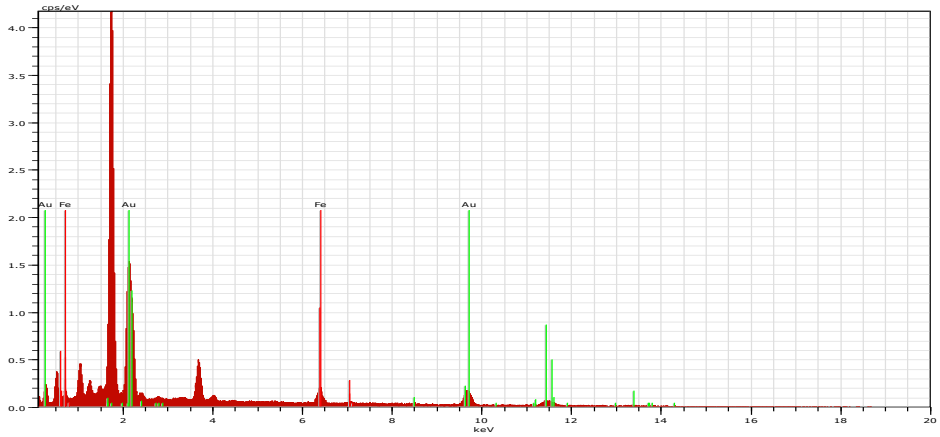


**Figure S4.** EDX analysis of the alloyed FeAu film.

**Table S1.** The estimated quantity of Fe and Au elements in the alloyed FeAu film.

| Element | norm. C (wt%) | atom. C (at%) | error (%) |
|---|---|---|---|
| Fe K | 10.09 | 28.35 | 0.2 |
| Au L | 89.91 | 71.65 | 1.8 |

It should be noted that the EDX analysis of the FeAu film shows the existence of Fe and/or Fe-compound. However, the XRD analysis of the film shows the presence predominantly of Au and Au-enriched FeAu alloy. This makes us conclude that the rest of the Fe probably participates in the amorphous compound.

The XPS analysis of the alloyed film surface is presented in Figure S5. The binding energy positions of the $Fe2p_{3/2}$ and Fe3p peaks, the spin-orbit splitting of 13.6 eV, and the presence of a satellite peak at about 719 eV are evidence that the Fe atoms were mainly in the $Fe^{3+}$ oxidation state Fe [34]. Here, it should be noted that a weak peak at 706.8 eV was also observed, which corresponds to metallic $Fe^0$ [34,36]. Further, the presence of Au was confirmed by registering the characteristic Au4f peak at a binding energy of 83.6 eV and a spin-orbit splitting of 3.7 eV. The lower binding energies of Au4f compared to the bulk Au indicate the formation of an FeAu alloy (Figure S5) [37,38]. The Fe: Au ratio at the surface was estimated to be 60:40. It could be concluded that the surface of the alloyed FeAu film was covered by the iron oxide phase.

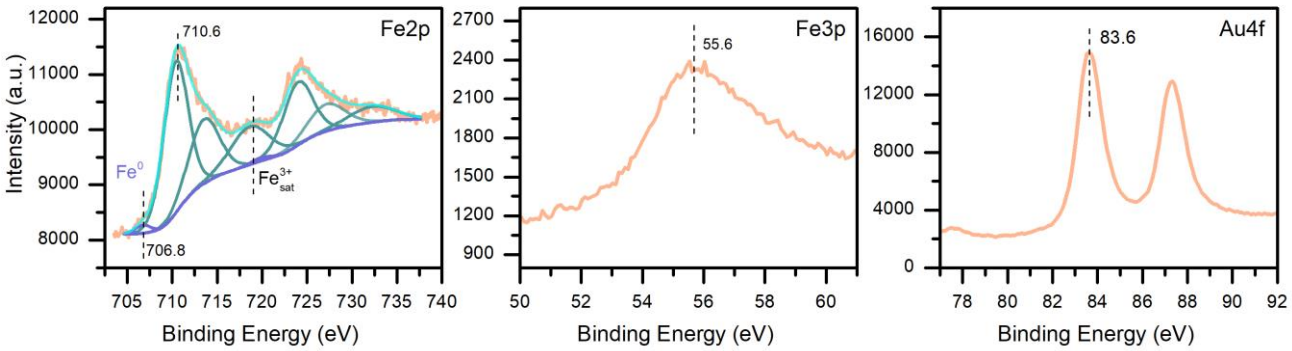


**Figure S5.** XPS spectra of the alloyed FeAu film.

*2. Elemental analyses of the nanostructures deposited from alloyed FeAu film.*

2.1. EDX analyses of the structures formed by *ns* ablation of alloyed FeAu film.

Figure S6 presents the EDX analysis of the structure deposited by *ns* ablation of the alloyed FeAu film. The estimated quantity of Fe and Au in the structure is shown in Table S2.

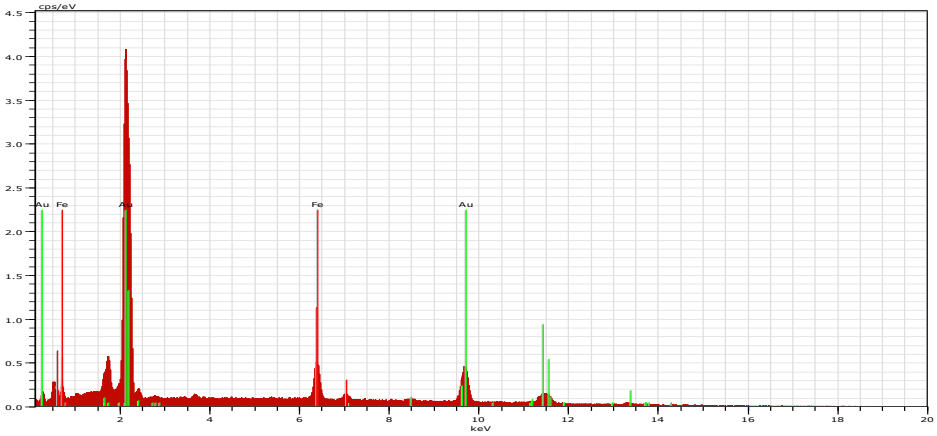


**Figure S6.** EDX analysis of the structure deposited by *ns* ablation of the alloyed FeAu film.

**Table S2.** The estimated Fe and Au quantity in the structure deposited by *ns* ablation.

| Element | norm. C (wt%) | atom. C (at%) | error (%) |
|---|---|---|---|
| Fe K | 12.06 | 32.60 | 0.3 |
| Au L | 87.94 | 67.40 | 2.4 |

2.2. EDX analyses of the structures formed by ps ablation of alloyed FeAu film.

Figure S7 shows the EDX analysis of the structure deposited by *ps* ablation of the alloyed FeAu film. The estimated quantity of Fe and Au in the structure is presented in Table S3.

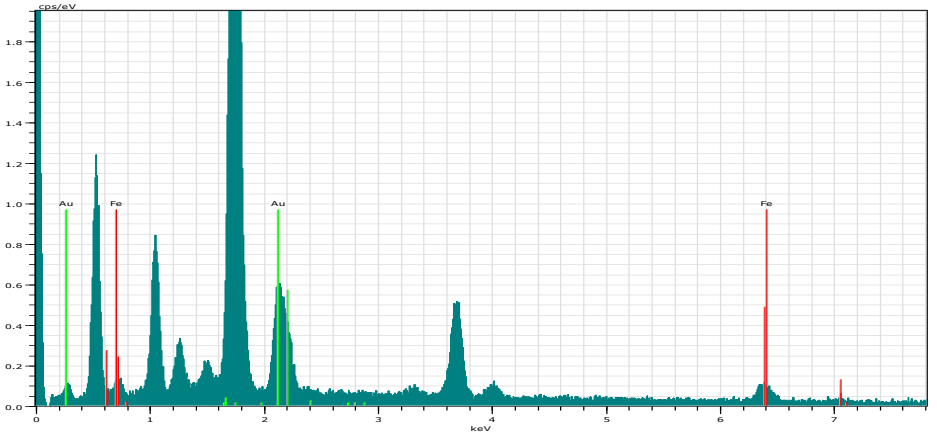


**Figure S7.** EDX analysis of the structure deposited by *ps* ablation of the alloyed FeAu film.

**Table S3.** The estimated Fe and Au quantity in the structure deposited by *ps* ablation.

| Element | norm. C (wt%) | atom. C (at%) | error (%) |
|---|---|---|---|
| Fe K | 14.93 | 38.23 | 0.2 |
| Au L | 85.07 | 61.77 | 1.1 |

*3. Optical properties of the nanostructures deposited from pure Fe and Au films by ns and ps ablation.*

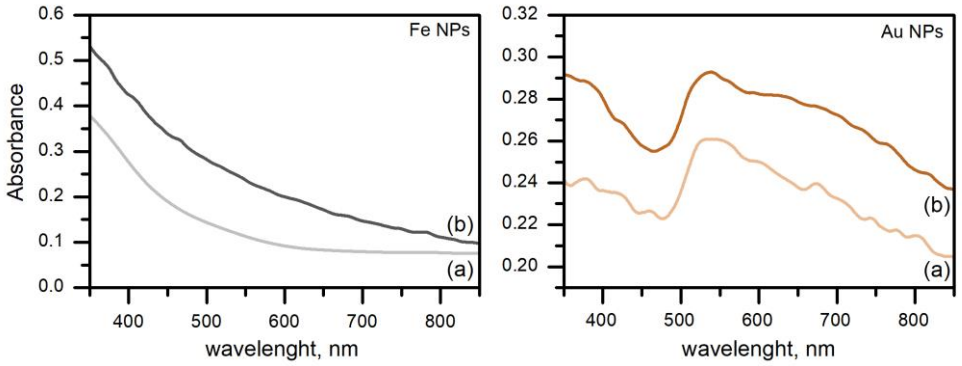


**Figure S8.** Optical properties of the samples deposited from pure Fe and Au films by (a) *ns* and (b) *ps* ablation.